2021

Quantifying 210Po/210Pb disequilibrium in seawater: A comparison of two precipitation methods with differing results

Montserrat Roca-Martí

Viena Puigcorbé
Edith Cowan University

Maxi Castrillejo

Núria Casacuberta

Jordi Garcia-Orellana

See next page for additional authors

10.3389/fmars.2021.684484
Roca-Martí, M., Puigcorbé, V., Castrillejo, M., Casacuberta, N., Garcia-Orellana, J., Cochran, J. K., & Masqué, P. (2021). Quantifying 210Po/210Pb disequilibrium in seawater: A comparison of two precipitation methods with differing results. *Frontiers in Marine Science, 8,* article 684484.https://doi.org/10.3389/fmars.2021.684484

frontiers in Marine Science

ORIGINAL RESEARCH
published: 22 June 2021
doi: 10.3389/fmars.2021.684484

Quantifying ^{210}Po/^{210}Pb Disequilibrium in Seawater: A Comparison of Two Precipitation Methods With Differing Results

Montserrat Roca-Martí[1,2], Viena Puigcorbé[3], Maxi Castrillejo[4], Núria Casacuberta[4], Jordi Garcia-Orellana[5,6], J. Kirk Cochran[7] and Pere Masqué[3,5,6,8]*

[1] Department of Marine Chemistry and Geochemistry, Woods Hole Oceanographic Institution, Woods Hole, MA, United States, [2] Department of Oceanography, Dalhousie University, Halifax, NS, Canada, [3] Centre for Marine Ecosystems Research, School of Science, Edith Cowan University, Joondalup, WA, Australia, [4] Laboratory of Ion Beam Physics, ETH Zürich, Zurich, Switzerland, [5] Institut de Ciència i Tecnologia Ambientals, Universitat Autònoma de Barcelona, Bellaterra, Spain, [6] Departament de Física, Universitat Autònoma de Barcelona, Bellaterra, Spain, [7] School of Marine and Atmospheric Sciences, Stony Brook University, Stony Brook, NY, United States, [8] International Atomic Energy Agency, Principality of Monaco, Monaco

OPEN ACCESS

Edited by:
Eric 'Pieter Achterberg, GEOMAR Helmholtz Centre for Ocean Research Kiel, Germany

Reviewed by:
Michiel Rutgers van der Loeff, Alfred Wegener Institute, Helmholtz Centre for Polar and Marine Research (AWI), Germany
Walter Geibert, Alfred Wegener Institute, Helmholtz Centre for Polar and Marine Research (AWI), Germany

***Correspondence:**
Montserrat Roca-Martí
mrocamarti@whoi.edu;
mrocamarti@dal.ca

Specialty section:
This article was submitted to Marine Biogeochemistry, a section of the journal Frontiers in Marine Science

Received: *23 March 2021*
Accepted: *11 May 2021*
Published: *22 June 2021*

Citation:
Roca-Martí M, Puigcorbé V, Castrillejo M, Casacuberta N, Garcia-Orellana J, Cochran JK and Masqué P (2021) Quantifying ^{210}Po/^{210}Pb Disequilibrium in Seawater: A Comparison of Two Precipitation Methods With Differing Results. Front. Mar. Sci. 8:684484. doi: 10.3389/fmars.2021.684484

The disequilibrium between lead-210 (^{210}Pb) and polonium-210 (^{210}Po) is increasingly used in oceanography to quantify particulate organic carbon (POC) export from the upper ocean. This proxy is based on the deficits of ^{210}Po typically observed in the upper water column due to the preferential removal of ^{210}Po relative to ^{210}Pb by sinking particles. Yet, a number of studies have reported unexpected large ^{210}Po deficits in the deep ocean indicating scavenging of ^{210}Po despite its radioactive mean life of ∼ 200 days. Two precipitation methods, $Fe(OH)_3$ and Co-APDC, are typically used to concentrate Pb and Po from seawater samples, and deep ^{210}Po deficits raise the question whether this feature is biogeochemically consistent or there is a methodological issue. Here, we present a compilation of ^{210}Pb and ^{210}Po studies that suggests that ^{210}Po deficits at depths >300 m are more often observed in studies where $Fe(OH)_3$ is used to precipitate Pb and Po from seawater, than in those using Co-APDC (in 68 versus 33% of the profiles analyzed for each method, respectively). In order to test whether ^{210}Po/^{210}Pb disequilibrium can be partly related to a methodological artifact, we directly compared the total activities of ^{210}Pb and ^{210}Po in four duplicate ocean depth-profiles determined by using $Fe(OH)_3$ and Co-APDC on unfiltered seawater samples. While both methods produced the same ^{210}Pb activities, results from the Co-APDC method showed equilibrium between ^{210}Pb and ^{210}Po below 100 m, whereas the $Fe(OH)_3$ method resulted in activities of ^{210}Po significantly lower than ^{210}Pb throughout the entire water column. These results show that ^{210}Po deficits in deep waters, but also in the upper ocean, may be greater when calculated using a commonly used

$Fe(OH)_3$ protocol. This finding has potential implications for the use of the ^{210}Po/^{210}Pb pair as a tracer of particle export in the oceans because ^{210}Po (and thus POC) fluxes calculated using $Fe(OH)_3$ on unfiltered seawater samples may be overestimated. Recommendations for future research are provided based on the possible reasons for the discrepancy in ^{210}Po activities between both analytical methods.

Keywords: marine chemistry, radiochemistry, polonium isotopes, precipitation methods, Co-APDC, $Fe(OH)_3$, ^{210}Po/^{210}Pb disequilibrium, particle export

INTRODUCTION

The biological carbon pump is a major mechanism for removing carbon dioxide from the atmosphere principally mediated by the transfer of organic particles from the surface to the deep ocean by different export pathways (Boyd et al., 2019). The flux of particulate organic carbon (POC) varies strongly across regions and time (Buesseler and Boyd, 2009), hindering the estimation of POC export in the global ocean (ranging from 5 to >12 Pg C yr^{-1}; Boyd and Trull, 2007; Henson et al., 2011; Siegel et al., 2014). The naturally occurring radionuclides lead-210 (^{210}Pb, half-life = 22.3 years) and polonium-210 (^{210}Po, half-life = 138 days) have been widely used as particle tracers in the marine environment for decades (e.g., Bacon et al., 1976, 1988; Cochran and Masqué, 2003) and, in the last years, especially, to quantify POC export (e.g., Tang and Stewart, 2019). Indeed, the combination of ^{210}Po/^{210}Pb with other particle export methods, such as sediment traps or the thorium-234/uranium-238 (^{234}Th/^{238}U) pair, has given a broader perspective on downward export fluxes integrating time scales ranging from a few days to several months (Stewart et al., 2007, 2011; Buesseler et al., 2008; Verdeny et al., 2009; Wei et al., 2011; Le Moigne et al., 2013; Ceballos-Romero et al., 2016; Maiti et al., 2016; Roca-Martí et al., 2016; Anand et al., 2018; Hayes et al., 2018).

The use of ^{210}Po/^{210}Pb disequilibrium as a proxy for POC export relies on the assumption that sinking of organic particles generates a deficit of ^{210}Po with respect to ^{210}Pb in the upper water column due to preferential scavenging of Po compared to Pb (Friedrich and Rutgers van der Loeff, 2002; Verdeny et al., 2009). Unlike ^{210}Pb (or ^{234}Th), Po can be assimilated into cells, possibly as an analog of sulfur, and subsequently cycled as the organic matter is regenerated (Stewart et al., 2008). In the particle-poor deep ocean, radioactive equilibrium between ^{210}Pb and ^{210}Po is anticipated because of the long scavenging residence times and short half-life of ^{210}Po (e.g., Bacon et al., 1976; Cochran et al., 1983). Yet, large deficits of ^{210}Po have been observed in the mesopelagic (~ 100–1000 m) and bathypelagic (>1000 m) zones in different regions of the world ocean, including the North Atlantic (e.g., Kim and Church, 2001; Hong et al., 2013; Rigaud et al., 2015), the North, Equatorial and South Pacific (e.g., Thomson and Turekian, 1976; Nozaki et al., 1990, 1997; Chung and Wu, 2005; Hu et al., 2014), the Arctic Ocean (e.g., Smith et al., 2003; Roca-Martí et al., 2018), and the Southern Ocean (e.g., Friedrich and Rutgers van der Loeff, 2002). Disequilibrium in deep waters has been commonly attributed to the scavenging of ^{210}Po by particles from the local upper water column or from the shelves due to high biological productivity (Hu et al., 2014; Rigaud et al., 2015; Ma et al., 2017). Recently, a model study by De Soto et al. (2018) has argued that the disequilibrium between ^{210}Pb and ^{210}Po at depth in the Porcupine Abyssal Plain, NE Atlantic, could be explained by a significant adsorption of ^{210}Po onto particles as they sink through the water column concurrent with negligible desorption. An alternate explanation is that this ^{210}Po deficit reflects a missing sink of ^{210}Po in deep waters by means, for instance, of ^{210}Po uptake by bacteria and its transfer to higher trophic levels in the oligotrophic ocean (Kim, 2001). Low ^{210}Po/^{210}Pb activity ratios at depth have also been associated with hydrothermal activity (Kadko et al., 1987) and the focusing of atmospherically derived ^{210}Pb (with low ^{210}Po) by isopycnal transport (Nozaki et al., 1990).

One hypothesis that has not been addressed yet is that these ^{210}Po deficits could also be influenced by an analytical bias. Church et al. (2012) pointed out that there is the potential for differential extraction of the Po spike used as a chemical yield tracer (usually ^{209}Po, although ^{208}Po has also been used) versus *in situ* ^{210}Po, depending on the precipitation method used. Two main methods have been used to pre-concentrate Pb and Po from seawater samples: the iron hydroxide [$Fe(OH)_3$, Thomson and Turekian, 1976] and the cobalt ammonium pyrrolidine dithiocarbamate (Co-APDC, Fleer and Bacon, 1984). The $Fe(OH)_3$ method is the most used analytical procedure for the extraction of ^{210}Pb and ^{210}Po from seawater likely because it is less time-consuming than the Co-APDC procedure. The latter method involves adding APDC to the sample to chelate Pb and Po and subsequent flocculation of the colloidal chelate by adding excess cobalt, followed by sample filtration. To date, studies have shown that both methods are effective in co-precipitating stable Pb and ^{209}Po added to seawater samples as yield monitors, as shown by recoveries of more than 70% of these spikes (Matthews et al., 2007; Rigaud et al., 2013). However, to our knowledge, there has been no systematic evaluation of whether the $Fe(OH)_3$ and Co-APDC methods produce comparable ^{210}Po results.

Here, we present a compilation of ^{210}Pb and ^{210}Po studies classified according to the precipitation method used and whether ^{210}Po deficits at depth were observed. In addition, we directly compare the total activities of ^{210}Pb and ^{210}Po in four duplicate ocean depth-profiles determined by using both precipitation methods, $Fe(OH)_3$ and Co-APDC, on unfiltered seawater samples. We discuss the implications of the results of

this comparison for using the ^{210}Po/^{210}Pb pair as a tracer of particle export in the oceans and provide recommendations for future research.

MATERIALS AND METHODS

Compilation of ^{210}Pb and ^{210}Po Studies

A review of ^{210}Pb and ^{210}Po studies was conducted in order to identify those that reported depth profiles of total (dissolved + particulate) ^{210}Pb and ^{210}Po activities in water depths >300 m, classify them according to the precipitation method used, and determine whether ^{210}Po deficits at depth were found (**Figure 1**). The compilation includes a total of 213 depth profiles from 41 studies published between 1976 and 2020.

The precipitation methods were divided into the following categories: (1) $Fe(OH)_{3\ TOT\ siph}$, where unfiltered seawater samples were precipitated with $Fe(OH)_3$ and the supernatant was siphoned off or decanted to allow further processing of the $Fe(OH)_3$ precipitate; (2) $Fe(OH)_{3\ TOT\ filt\ precip}$, where unfiltered seawater samples were precipitated with $Fe(OH)_3$ and the precipitate was filtered; (3) $Fe(OH)_{3\ DISS\ +\ PART}$, where prefiltered seawater samples were precipitated with $Fe(OH)_3$ and the particulate fraction was analyzed separately; (4) Co-APDC $_{TOT}$, where unfiltered seawater samples were precipitated with Co-APDC; (5) Co-APDC $_{DISS+PART}$, where prefiltered seawater samples were precipitated with Co-APDC and the particulate fraction was analyzed separately.

In addition, we determined whether ^{210}Po deficits at depth were found for those profiles that presented total ^{210}Pb and ^{210}Po activities at least at two depths from ≥300 m. Profiles were considered to show ^{210}Po deficits at depth if they presented total ^{210}Po/^{210}Pb activity ratios <0.8 at least at two depths ≥300 m.

Duplicate Profiles of ^{210}Pb and ^{210}Po

Detailed procedures for the methods compared in this study [$Fe(OH)_{3\ TOT\ siph}$ and Co-APDC $_{TOT}$ in **Figure 1**] are described below and can be found at the Center for Marine and Environmental Radioactivity website[1]. Additional details for each set of samples processed using $Fe(OH)_3$ and Co-APDC are provided in **Supplementary Table 1** including information on the ^{209}Po and stable Pb tracers, detector background, blank from the stable Pb tracer, and chemical recoveries.

Sampling and Pre-conditioning

A total of 35 duplicate sample pairs were collected for the determination of total ^{210}Pb and ^{210}Po in seawater (6.5–10.4 L, **Supplementary Table 1**) using Niskin bottles attached to a conductivity-temperature-depth (CTD) rosette at four locations (**Figure 2** and **Table 1**). Three profiles were collected in the Mediterranean Sea in 2011–2013 (Ionian and Catalano-Balear Seas), while another profile was collected at the Southern Ocean Time Series (SOTS) site in 2018. This allowed to increase the statistical significance and compare results obtained from contrasting oceanographic regimes. Duplicate samples were all collected from the same CTD cast and the same Niskin bottles, except for one profile (Catalano-Balear South, CBS) where duplicate samples were collected from different Niskin bottles.

Unfiltered seawater samples were acidified immediately after collection to pH 1–2 using HCl (∼ 1 mL per liter of sample), and spiked with known amounts of ^{209}Po ($T_{1/2}$ = 125 years, 2–4 dpm, **Supplementary Table 1**) and stable Pb (4–42 mg, **Supplementary Table 1**) to monitor the losses of Po and Pb during the radiochemistry procedure. Samples were vigorously shaken after the addition of HCl and each spike. Two solutions of ^{209}Po were used, both in acid media (9 M HCl for the Mediterranean Sea samples; 1 M HNO_3 for SOTS) and prepared from standard solutions (Oak Ridge National Laboratory, United States; Eckert & Ziegler, Germany; respectively). The Pb solution (aqueous) was prepared from ancient Pb (>200 years) to minimize ^{210}Pb and ^{210}Po contamination. From each pair of duplicates, one sample was processed using $Fe(OH)_3$ (Thomson and Turekian, 1976; Sarin et al., 1992) and the other using Co-APDC (Boyle and Edmond, 1975; Fleer and Bacon, 1984) as described below. All initial processing, including the precipitation of ^{210}Pb and ^{210}Po, was accomplished at sea.

Fe-Hydroxide Method

240 mg of Fe were added to each acidified and spiked sample in the form of $FeCl_3$ solution. After vigorous shaking, samples were allowed to equilibrate for 9–24 h (**Supplementary Table 1**). Pb and Po isotopes were then precipitated with $Fe(OH)_3$ by adjusting the pH to 8–9 with NH_4OH. The precipitate was allowed to settle for a few hours, and then most of the supernatant visibly free of iron hydroxides was carefully siphoned off. The precipitate was transferred into 250 mL plastic bottles and stored for 12–37 days (**Supplementary Table 1**) until further processing in land-based laboratories: Mediterranean Sea samples were analyzed at Universitat Autònoma de Barcelona and SOTS samples at the Edith Cowan University. There, samples were centrifuged and the excess supernatant removed. Milli-Q water was then added to the precipitates to dissolve salts and remove them by suction after a second centrifugation. Precipitates were transferred into beakers and dissolved using concentrated HCl. After evaporation to near dryness, samples were re-dissolved with ∼ 80 mL of 1 M HCl and ascorbic acid was added to reduce Fe^{3+} to Fe^{2+}.

Co-APDC Method

After 9–24 h of isotope equilibration, 10 mg of Co and 800 mg of APDC were added to each sample as cobalt nitrate and APDC solutions, shaking the samples vigorously after each reagent addition. Samples were allowed to equilibrate for several hours (6–12 h) and then filtered through 0.2 μm pore-size filters (Whatman membrane filters mixed cellulose ester, WHA10401731, 142 mm diameter). Samples were stored for later processing in the land-based laboratories. The filters with the Co-APDC precipitates were digested at <100°C using concentrated HNO_3 in beakers covered with watch glasses. The solutions were then evaporated to near dryness and HNO_3 was completely eliminated from the samples by addition of 2 mL of concentrated HCl and subsequent evaporation to near dryness

[1]https://cmer.whoi.edu/cookbook/

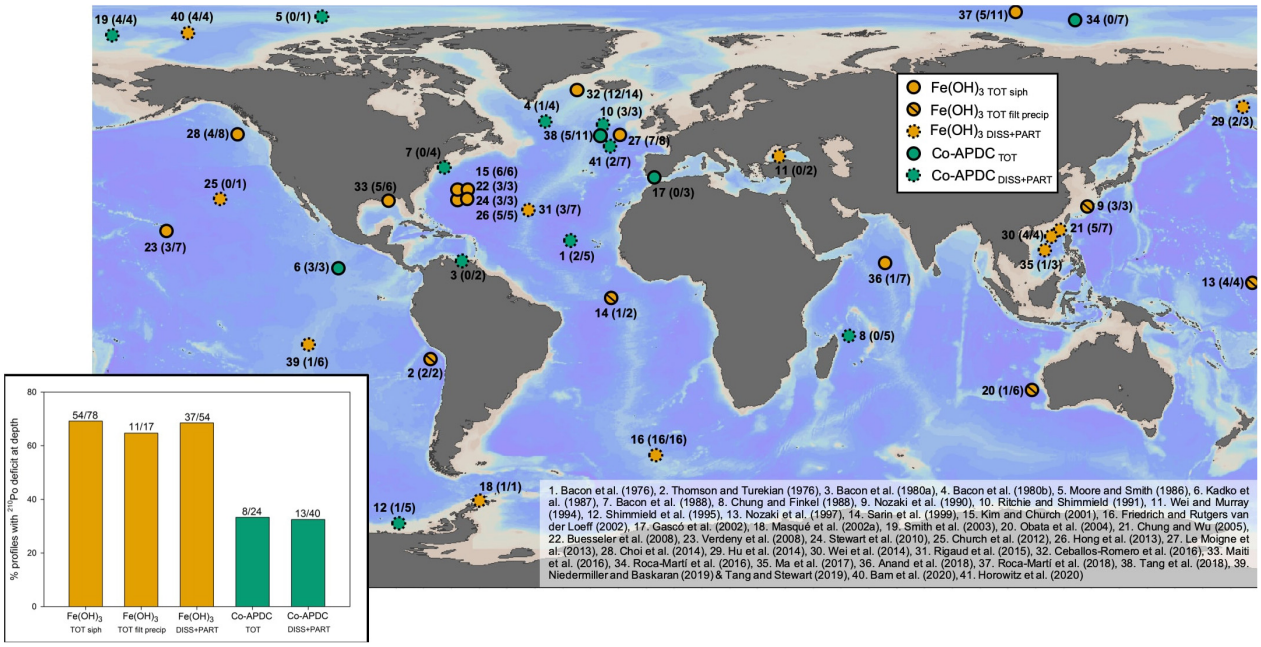

FIGURE 1 | Compilation of studies reporting depth profiles (≥300 m) of total ^{210}Pb and ^{210}Po activities. Legend shows the precipitation method used in each study: $Fe(OH)_{3\ TOT\ siph}$, $Fe(OH)_{3\ TOT\ filt\ precip}$, $Fe(OH)_{3\ DISS\ +\ PART}$, Co-APDC $_{TOT}$, Co-APDC $_{DISS+PART}$ (see section "Compilation of ^{210}Pb and ^{210}Po Studies" for definitions). Many of these studies represent a transect of stations but for clarity the dots represent the location of one of the stations sampled for ^{210}Pb and ^{210}Po per study. The number next to each dot corresponds to the study reference and the numbers in parentheses refer to the number of profiles where deficits of ^{210}Po (total ^{210}Po/^{210}Pb activity ratios <0.8) at depth were found, as shown by at least two data points from ≥300 m, with respect to the total profiles analyzed per study. The inset plot shows the percentage of profiles with deficits of ^{210}Po at depth with respect to the total profiles analyzed per method considering all studies compiled. To avoid duplication, data from the D341 cruise presented in Le Moigne et al. (2013) were excluded from the dataset presented in Ceballos-Romero et al. (2016); data from Roca-Martí et al. (2018) were obtained from a combination of unfiltered and prefiltered samples [$Fe(OH)_{3\ TOT\ siph}$ and $Fe(OH)_{3\ DISS\ +\ PART}$].

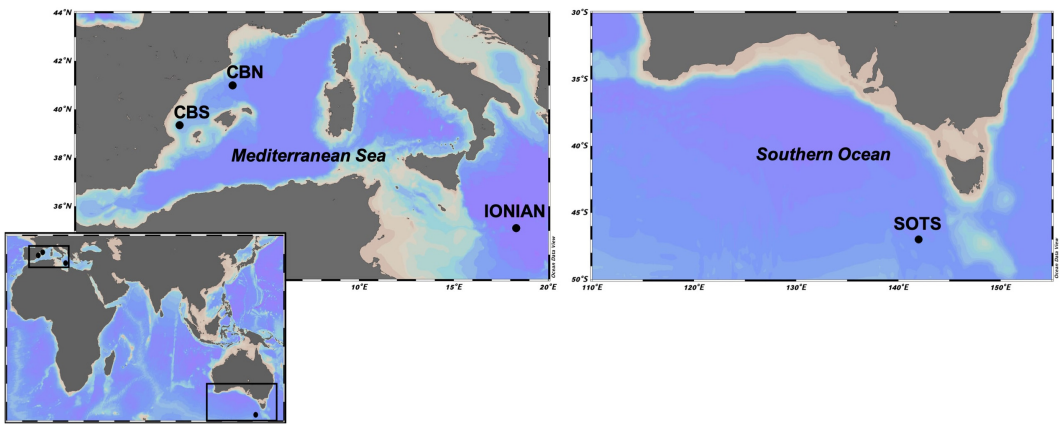

FIGURE 2 | Study areas where duplicate ocean depth-profiles were collected for total ^{210}Pb and ^{210}Po analyses in the Catalano-Balear (north: CBN; south: CBS) and Ionian Seas (left map), and at the Southern Ocean Time Series (SOTS) site (right map).

for three consecutive times. The residues were re-dissolved with ∼ 80 mL of 1 M HCl.

Po Plating and Counting

Silver disks (0.1 mm thick, 25 mm diameter) were suspended in the 1 M HCl solutions using a nylon string to allow the auto-deposition of Po isotopes (i.e., plating) at ∼ 80°C and constant stirring for at least 6 h (Flynn, 1968). One side of the disks was previously coated with urethane to maximize Po plating on the non-coated side and optimize counting statistics. The time elapsed between sampling and the first Po plating was minimized as much as possible to reduce the uncertainty of ^{210}Po activities (Rigaud et al., 2013). ^{210}Po and ^{209}Po emissions were counted by alpha spectrometry (Fleer and Bacon, 1984) using

TABLE 1 | Total ^{210}Pb and ^{210}Po activities and ^{210}Po/^{210}Pb activity ratios measured using the $Fe(OH)_3$ and Co-APDC precipitation methods [$Fe(OH)_{3\ TOT\ siph}$ and Co-APDC $_{TOT}$ protocols in **Figure 1**] in four duplicate ocean depth-profiles.

Study area*	Depth (m)	^{210}Pb (dpm 100 L^{-1})		^{210}Po (dpm 100 L^{-1})		^{210}Po/^{210}Pb	
		$Fe(OH)_3$	Co-APDC	$Fe(OH)_3$	Co-APDC	$Fe(OH)_3$	Co-APDC
IONIAN Mediterranean Sea 35.1°N, 18.3°E, 12 May 2013	10	10.5 ± 0.9	10.4 ± 0.8	6.6 ± 0.4	8.8 ± 0.6	0.63 ± 0.07	0.85 ± 0.09
	50	10.1 ± 0.8	9.3 ± 0.7	6.3 ± 0.4	8.0 ± 0.4	0.62 ± 0.06	0.86 ± 0.08
	75	10.4 ± 0.8	9.2 ± 0.7	5.5 ± 0.4	8.7 ± 0.5	0.53 ± 0.05	0.95 ± 0.09
	100	10.8 ± 0.8	7.5 ± 0.6	4.7 ± 0.3	7.4 ± 0.5	0.43 ± 0.05	0.99 ± 0.10
	500	7.7 ± 0.6	9.5 ± 0.7	3.8 ± 0.2	8.7 ± 0.5	0.50 ± 0.05	0.92 ± 0.09
	3720	8.9 ± 0.7	8.3 ± 0.7	6.9 ± 0.4	9.6 ± 0.6	0.77 ± 0.07	1.16 ± 0.11
CATALANO-BALEAR NORTH (CBN) Mediterranean Sea 41.0°N, 3.3°E, 31 May 2013	25	7.8 ± 0.6	7.2 ± 0.6	3.9 ± 0.2	4.3 ± 0.3	0.51 ± 0.05	0.60 ± 0.06
	50	8.5 ± 0.7	7.9 ± 0.6	3.3 ± 0.2	4.7 ± 0.3	0.39 ± 0.04	0.60 ± 0.06
	75	6.6 ± 0.5	6.5 ± 0.5	3.9 ± 0.2	5.9 ± 0.4	0.59 ± 0.06	0.91 ± 0.10
	100	7.1 ± 0.6	6.7 ± 0.6	4.6 ± 0.3	6.3 ± 0.3	0.64 ± 0.07	0.94 ± 0.09
	250	6.4 ± 0.5	6.4 ± 0.5	4.6 ± 0.3	5.5 ± 0.3	0.72 ± 0.07	0.86 ± 0.09
	500	6.2 ± 0.5	6.7 ± 0.5	4.7 ± 0.3	6.5 ± 0.4	0.75 ± 0.08	0.97 ± 0.09
	750	8.0 ± 0.7	7.4 ± 0.6	6.3 ± 0.3	6.4 ± 0.4	0.78 ± 0.08	0.88 ± 0.09
	1000	7.1 ± 0.6	9.1 ± 0.7	6.1 ± 0.3	8.1 ± 0.5	0.86 ± 0.08	0.89 ± 0.09
	1500	7.5 ± 0.6	6.5 ± 0.5	6.5 ± 0.3	6.0 ± 0.3	0.87 ± 0.08	0.93 ± 0.09
	2200	6.8 ± 0.5	6.0 ± 0.5	5.2 ± 0.3	6.4 ± 0.4	0.76 ± 0.07	1.08 ± 0.11
CATALANO-BALEAR SOUTH (CBS) Mediterranean Sea 39.3-39.4°N, 0.4-0.6°E, 11 Feb 2011	50	7.2 ± 0.7	7.1 ± 0.6	3.9 ± 0.4	3.4 ± 0.4	0.53 ± 0.08	0.48 ± 0.07
	125	6.9 ± 0.6	6.1 ± 0.6	1.5 ± 0.3	3.1 ± 0.4	0.21 ± 0.05	0.51 ± 0.08
	250	8.9 ± 0.8	8.1 ± 0.8	1.7 ± 0.4	4.6 ± 0.5	0.19 ± 0.05	0.58 ± 0.08
	400	8.2 ± 0.7	7.2 ± 0.6	3.8 ± 0.4	5.1 ± 0.6	0.46 ± 0.06	0.72 ± 0.10
	950	10.1 ± 0.8	8.9 ± 0.8	4.1 ± 0.4	6.5 ± 0.6	0.41 ± 0.05	0.73 ± 0.09
	1200	9.4 ± 0.8	10.7 ± 0.8	3.6 ± 0.5	6.4 ± 0.7	0.38 ± 0.06	0.60 ± 0.08
Southern Ocean Time Series (SOTS) 47.0°S, 142.0°E, 5 March 2018	25	12.9 ± 0.8	11.8 ± 0.8	7.5 ± 0.6	7.6 ± 0.6	0.59 ± 0.06	0.64 ± 0.06
	50	10.9 ± 0.7	10.4 ± 0.6	7.2 ± 0.5	9.4 ± 0.7	0.66 ± 0.06	0.91 ± 0.09
	80	13.0 ± 0.8	11.8 ± 0.7	6.1 ± 0.5	10.4 ± 0.8	0.46 ± 0.05	0.89 ± 0.09
	100	13.3 ± 0.8	12.9 ± 0.8	5.0 ± 0.5	13.8 ± 1.0	0.37 ± 0.04	1.08 ± 0.10
	125	14.5 ± 0.8	13.1 ± 0.7	5.9 ± 0.6	15.1 ± 1.1	0.41 ± 0.05	1.16 ± 0.11
	150	12.8 ± 0.8	12.7 ± 0.7	7.2 ± 0.6	11.2 ± 0.8	0.56 ± 0.06	0.89 ± 0.08
	200	13.5 ± 0.8	13.6 ± 0.8	5.0 ± 0.4	12.2 ± 0.9	0.37 ± 0.04	0.90 ± 0.08
	300	13.5 ± 0.8	14.1 ± 0.8	5.6 ± 0.5	13.5 ± 0.8	0.41 ± 0.04	0.95 ± 0.08
	400	12.6 ± 0.8	13.1 ± 0.8	6.3 ± 0.5	11.6 ± 0.7	0.49 ± 0.05	0.89 ± 0.07
	800	12.0 ± 0.7	13.4 ± 0.8	7.4 ± 0.6	12.5 ± 0.9	0.61 ± 0.06	0.94 ± 0.08
	1000	11.7 ± 0.7	12.7 ± 0.7	8.3 ± 0.6	14.2 ± 0.9	0.71 ± 0.07	1.12 ± 0.10
	1200	14.5 ± 0.8	16.7 ± 0.8	10.3 ± 0.8	13.5 ± 0.8	0.71 ± 0.06	0.81 ± 0.06
	1600	14.3 ± 0.7	15.5 ± 0.8	13.5 ± 1.0	16.2 ± 1.0	0.95 ± 0.09	1.04 ± 0.08

**Primary production zone depth was 175 m at IONIAN, 90 m at CBN, 156 m at CBS, and 102 m at SOTS. Water column depth was 3775 m at IONIAN, 2274 m at CBN, 1262 m at CBS, and 4600 m at SOTS.*

passivated implanted planar silicon alpha detectors (Canberra, United States) or silicon surface barrier alpha detectors (EG&G Ortec, United States). The disks were counted until a minimum of 400 counts of both isotopes were accumulated or up to a maximum of 5 days. The detector background contributed on average to <1% of the total counts of ^{209}Po and ^{210}Po (**Supplementary Table 1**). The recoveries of the ^{209}Po tracer averaged 78 ± 8% for the $Fe(OH)_3$ method and 63 ± 16% for Co-APDC (Mann–Whitney rank-sum test, $P \leq 0.001$; **Supplementary Table 1**). Solutions were re-plated and also passed through an anion-exchange resin (AG 1-X8, Sarin et al., 1992) to ensure the complete elimination of Po from samples (Rigaud et al., 2013). Samples were re-spiked with 2–4 dpm of ^{209}Po tracer and stored for at least 6 months in 9 M HCl to allow ^{210}Po ingrowth from ^{210}Pb. After this time, samples were evaporated to near-dryness and re-dissolved with 1 M HCl to determine ^{210}Po ingrowth from ^{210}Pb by re-plating the solutions on silver disks and subsequent measurement of Po isotopes by alpha spectrometry as described above.

Chemical Recoveries of Pb and Data Treatment

Typically, two aliquots from each sample were taken before the first and last platings to determine the chemical recovery of stable Pb by inductively coupled plasma-optical emission spectrometry. However, only the second aliquot was taken from CBS samples. Considering all other samples, the recovery of Pb

from the first aliquot was on average 89 ± 7% for the $Fe(OH)_3$ method and 78 ± 12% for Co-APDC (Mann–Whitney rank-sum test, $P \leq 0.001$; **Supplementary Table 1**). These results were not significantly different from those determined from the second aliquot [Mann–Whitney rank-sum test, $P = 0.276$ for $Fe(OH)_3$ and $P = 0.401$ for Co-APDC; **Supplementary Figure 1**], indicating that Pb losses occurred during the precipitation with $Fe(OH)_3$ or Co-APDC rather than during the anion-exchange procedure. Therefore, for CBS samples, we assumed that the Pb recoveries at the first plating were the same as those determined at the last plating.

The ^{210}Pb and ^{210}Po blanks measured were equivalent to 0.014–0.016 dpm for the Ionian, Catalano-Balear North (CBN) and SOTS profiles. They increased to 0.270 dpm for the CBS profile due to the higher amount of stable Pb added. The contamination from the Pb solution contributed on average to <4% of the ^{210}Po activity at the first and last platings, except for the CBS profile, where it contributed 25–32% (**Supplementary Table 1**).

^{210}Pb and ^{210}Po activities at the time of sampling were carefully calculated applying blank, ingrowth, decay and recovery corrections, as detailed by Rigaud et al. (2013). Overall uncertainties in activity accounting for errors in counting, detector background, ^{209}Po activity, and the contamination from the Pb solution were on average 7% for ^{210}Pb (5–10%) and 8% for ^{210}Po (5–23%) for both methods.

Three-way ANOVA tests were run in order to examine whether $Fe(OH)_3$ and Co-APDC resulted in comparable ^{210}Pb and ^{210}Po results and whether potential methodological differences depended on the region or water depth [see section "Direct Comparison of the $Fe(OH)_3$ versus Co-APDC Methods"]. The factors considered were: (i) precipitation method [$Fe(OH)_3$ versus Co-APDC]; (ii) region (Mediterranean Sea versus SOTS); (iii) depth (within the primary production zone versus deeper waters). The base of the primary production zone (PPZ) was defined as the depth where fluorescence declined to 10% of the maximum signal measured in overlying waters (Owens et al., 2015). Statistical analyses were conducted using SigmaPlot 11.0 (Systat Software, Inc., United States) with a significance level set at 0.05.

RESULTS

Compilation of ^{210}Pb and ^{210}Po Studies

Two-thirds of the ^{210}Pb and ^{210}Po studies in the literature compilation (**Figure 1**) used the $Fe(OH)_3$ method, of which 59% analyzed total activities from unfiltered seawater samples [$Fe(OH)_{3\ TOT}$], while the remaining analyzed the dissolved and particulate fractions separately [$Fe(OH)_{3\ DISS\ +\ PART}$]. Most of the $Fe(OH)_3$ studies that measured total ^{210}Pb and ^{210}Po siphoned off or decanted the supernatant to allow further processing of the $Fe(OH)_3$ precipitate [$Fe(OH)_{3\ TOT\ siph}$], while some filtered the precipitate [$Fe(OH)_{3\ TOT\ filt\ precip}$]. Almost all the studies that prefiltered the samples siphoned off or decanted the supernatant from the samples as well. The other third of the ^{210}Pb and ^{210}Po studies used the Co-APDC method, of which 71% separated the dissolved and particulate fractions (Co-APDC $_{DISS+PART}$), while the remaining measured total ^{210}Pb and ^{210}Po from unfiltered samples (Co-APDC $_{TOT}$). All the Co-APDC studies filtered the precipitate.

In addition to classifying the studies according to the method used, we also determined whether ^{210}Po deficits (total ^{210}Po/^{210}Pb activity ratios <0.8) were found. Interestingly, this compilation shows that ^{210}Po deficits at depths ≥300 m are found in 65–69% of the profiles analyzed using $Fe(OH)_3$, while they are found in only 33% of the profiles analyzed using Co-APDC (**Figure 1**). This finding is independent of whether ^{210}Pb and ^{210}Po were analyzed on unfiltered or prefiltered seawater samples.

Duplicate Profiles of ^{210}Pb and ^{210}Po

^{210}Pb and ^{210}Po Activities

The profiles of ^{210}Pb and ^{210}Po determined using $Fe(OH)_3$ [$Fe(OH)_{3\ TOT\ siph}$] and Co-APDC (Co-APDC $_{TOT}$) in duplicate samples collected from the same CTD cast are shown in **Figure 3** (see data in **Table 1**). ^{210}Pb activities were not statistically different between both methods, ranging from 6.0–6.2 to 10.7–10.8 dpm 100 L^{-1} in the Mediterranean Sea (t-test, $P = 0.122$), and from 10.4–10.9 to 14.5–16.7 dpm 100 L^{-1} at SOTS (t-test, $P = 0.572$). In contrast, ^{210}Po activities were significantly different. In the Mediterranean Sea, ^{210}Po activities ranged from 1.5 to 6.9 dpm 100 L^{-1} for $Fe(OH)_3$ and from 3.1 to 9.6 dpm 100 L^{-1} for Co-APDC (t-test, $P < 0.001$; Ionian, CBN and CBS in **Figure 3B** and **Table 1**). In the Southern Ocean, at SOTS, ^{210}Po activities ranged from 5.0 to 13.5 dpm 100 L^{-1} for $Fe(OH)_3$ and from 7.6 to 16.2 dpm 100 L^{-1} for Co-APDC (t-test, $P < 0.001$). The higher activities of both radionuclides at SOTS reflect the higher levels of their grandparent, ^{226}Ra, in the Southern Ocean compared to the Mediterranean Sea (Ku and Lin, 1976; van Beek et al., 2009).

The $Fe(OH)_3$ results showed deficits of ^{210}Po at all sites and throughout the entire profiles. Below the PPZ, activities of ^{210}Po were lower than ^{210}Pb on average by a factor of 1.9 and equilibrium between both radionuclides was only observed at 1600 m at SOTS (**Figure 3B**). On the contrary, results from Co-APDC showed net removal of ^{210}Po confined in the upper 75–100 m (**Figure 3A**), and similar ^{210}Pb and ^{210}Po activities at deeper depths. In general, ^{210}Pb and ^{210}Po from Co-APDC reached equilibrium around the PPZ depth (**Figure 3A**). This is in line with recent studies that found a close overlap between the PPZ depth and the horizon where the ^{234}Th/^{238}U radionuclide pair reaches equilibrium (Puigcorbé et al., 2017; Roca-Martí et al., 2017; Lemaitre et al., 2018; Buesseler et al., 2020a,b). There is, however, one exception to this pattern. At CBS, ^{210}Po activities were lower than ^{210}Pb activities throughout the entire profile for both methods (**Figure 3B**). Consequently, ^{210}Po/^{210}Pb activity ratios were lower than 1.0 within the PPZ and in deeper waters, averaging 0.37 ± 0.14 for $Fe(OH)_3$ and 0.60 ± 0.10 for Co-APDC (**Figure 4** and **Table 1**). In this area of the Mediterranean Sea, turbidity spikes were observed throughout the entire water column below the surface maximum (**Supplementary Figure 2**), suggesting a possible net removal of ^{210}Po by particles below the PPZ in such conditions. At the

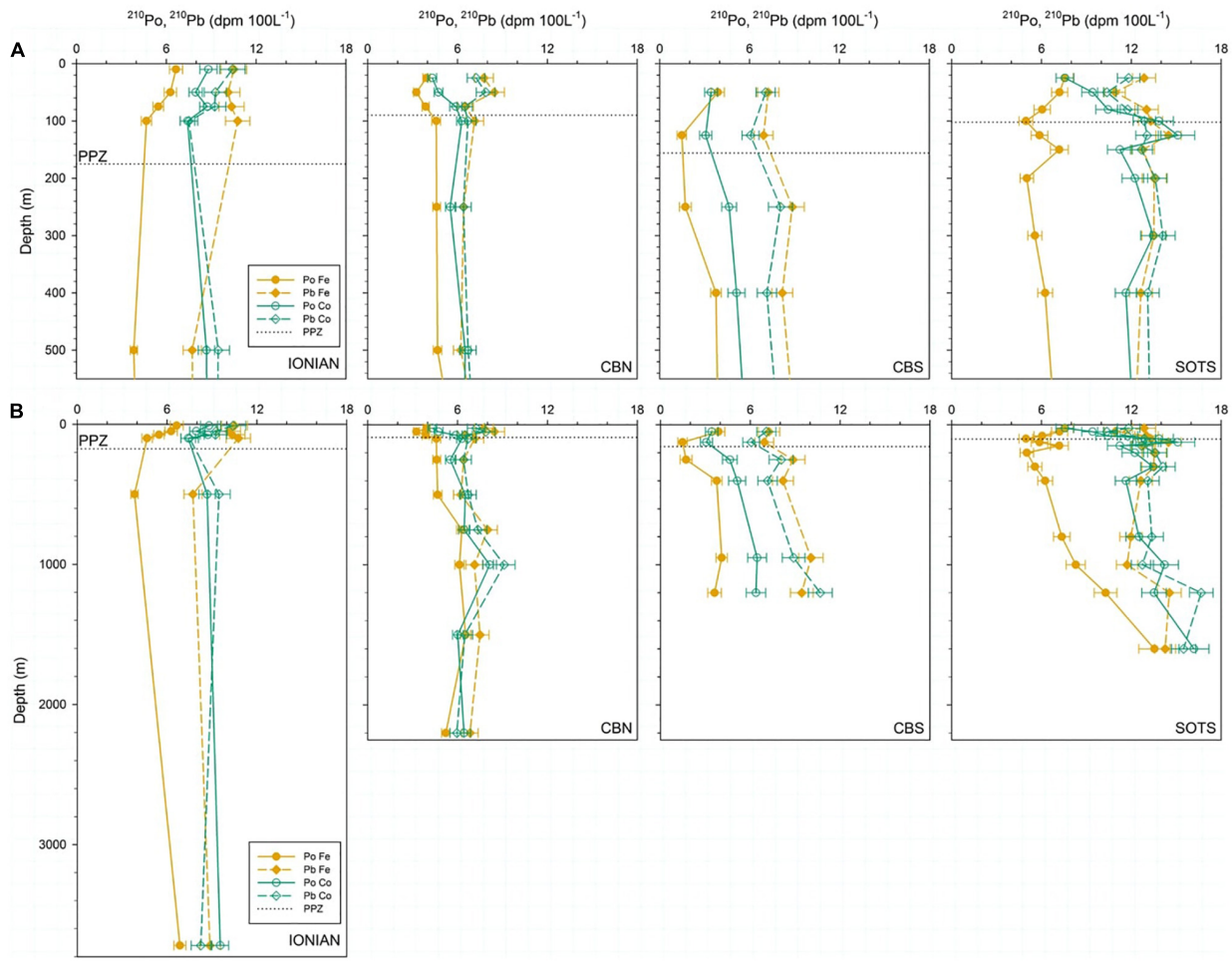

FIGURE 3 | Vertical activity profiles for total ^{210}Po (solid lines) and total ^{210}Pb (dashed lines) measured in duplicate samples using the $Fe(OH)_3$ (yellow, closed symbols) and Co-APDC (green, open symbols) precipitation methods [$Fe(OH)_{3\ TOT\ siph}$ and Co-APDC $_{TOT}$ protocols in **Figure 1**]. **(A)** Shows only the upper 500 m of the water column, while **(B)** shows the entire profiles. Same scale is used for the *x*- and *y*-axis to facilitate comparison. The base of the primary production zone (PPZ) is denoted by the horizontal dotted line.

other stations, turbidity spikes below the surface were not as pronounced as at CBS.

The ^{210}Po/^{210}Pb activity ratios (**Figure 4**) from both methods were statistically different (*t*-test, $P < 0.001$) with mean values from surface waters to the PPZ depth of 0.53 ± 0.10 using $Fe(OH)_3$ and 0.84 ± 0.16 using Co-APDC, and 0.66 ± 0.17 and 0.96 ± 0.10, respectively, below the PPZ excluding the CBS profile.

Direct Comparison of the $Fe(OH)_3$ versus Co-APDC Methods

Figure 5 shows a cross-plot of the ^{210}Pb and ^{210}Po activities obtained from the $Fe(OH)_3$ and Co-APDC methods. ^{210}Pb results from Co-APDC and $Fe(OH)_3$ were statistically similar (ANOVA test, $P = 0.418$ for the entire dataset, 0.263 for the Mediterranean and 0.849 for SOTS; **Figure 5**) with differences between mean activities of only 0.2–0.4 dpm 100 L^{-1} for the entire dataset. There was no significant difference between methods either when comparing samples within the PPZ or below (ANOVA test, $P = 0.151$ and $P = 0.536$, respectively). This agrees with the experiments conducted by Chung et al. (1983) in which $Fe(OH)_3$ and Co-APDC produced identical ^{210}Pb results. Chung et al. (1983) also tested the effect of equilibration times between ^{210}Pb and the added stable Pb carrier for times ranging from 1 to 330 days. Their results showed no discernible effect on the measured ^{210}Pb activities.

In contrast, ^{210}Po activities from samples processed using Co-APDC were significantly higher than those obtained by using $Fe(OH)_3$ (ANOVA test, $P < 0.001$; **Figure 5**). The difference in the mean ^{210}Po activities observed between the two precipitation methods was 3.0 dpm 100 L^{-1} for the entire dataset [Co-APDC: 8.6 ± 3.6 dpm 100 L^{-1}; $Fe(OH)_3$: 5.6 ± 2.3 dpm 100 L^{-1}], which corresponds to 35% of the ^{210}Po activity obtained with the Co-APDC method. The same statistical analysis was applied separately for the Mediterranean Sea profiles and SOTS (ANOVA test, $P = 0.003$ and $P < 0.001$, respectively), showing

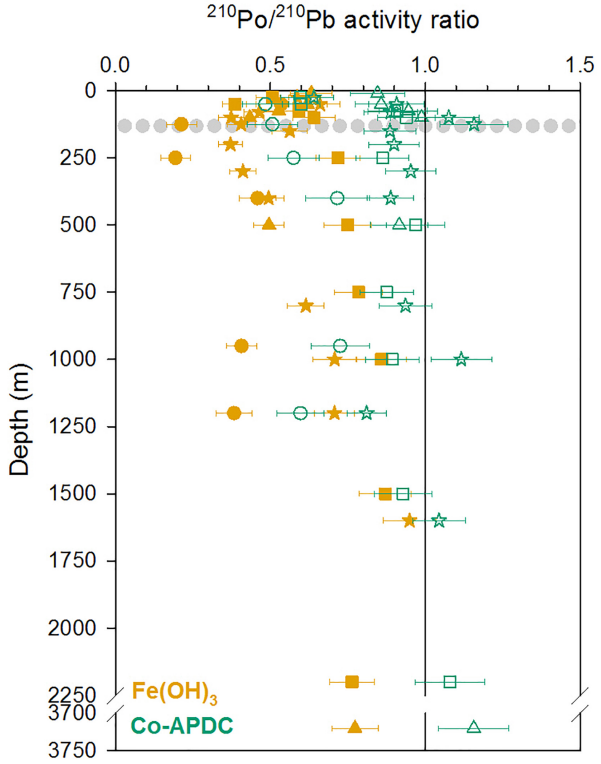

FIGURE 4 | ^{210}Po/^{210}Pb activity ratio determined by using the Fe(OH)$_3$ (yellow, closed symbols) and Co-APDC (green, open symbols) methods. Symbols denote different study areas: IONIAN (triangles), CBN (squares), CBS (circles), and SOTS (stars). The vertical solid line indicates ^{210}Po/^{210}Pb activity ratio = 1.0, and the horizontal dotted line is the average depth of the primary production zone in the study areas.

that the difference in absolute and relative terms between the two methods was larger in the Southern Ocean. At SOTS the difference was 5.1 dpm 100 L^{-1}, equivalent to 41% of the ^{210}Po activity obtained with the Co-APDC method, while in the Mediterranean Sea these values were 1.8 dpm 100 L^{-1} and 28%, respectively. Further, the use of Co-APDC resulted in higher ^{210}Po activities both within the PPZ and in deeper waters (ANOVA test, $P < 0.001$ for both; **Figure 5**), obtaining a difference between methods equal to 32% and 36% of the ^{210}Po activity obtained with the Co-APDC method, respectively.

Our results from four duplicate ^{210}Pb and ^{210}Po profiles support that either scavenging method can be used for reliably extracting ^{210}Pb from seawater, but the Fe(OH)$_{3\ \mathrm{TOT\ siph}}$ method underestimates ^{210}Po activities.

DISCUSSION

Possible Reasons for the Discrepancy in ^{210}Po Between Methods

The compilation of ^{210}Pb and ^{210}Po studies summarized in **Figure 1** suggests that the Fe(OH)$_3$ and Co-APDC methods may yield disparate results for ^{210}Po. As these studies are from different oceanographic regimes and were conducted at different times, a direct comparison of methods is difficult. However, the total ^{210}Pb and ^{210}Po activity results presented here from four duplicate profiles indicate that the Fe(OH)$_{3\ \mathrm{TOT\ siph}}$ method underestimated ^{210}Po activities throughout the entire water column. ^{210}Po activities are calculated from the ratio between the count rate of ^{210}Po to ^{209}Po multiplied by the known activity of ^{209}Po added to the samples, and applying appropriate ingrowth and decay corrections (Rigaud et al., 2013). Therefore, while similarly high ^{209}Po recoveries were obtained for both methods [78 ± 8% for Fe(OH)$_3$ and 63 ± 16% for Co-APDC], ^{210}Po was scavenged differently. Below we discuss two possible hypotheses that could explain how the Fe(OH)$_3$ method may have resulted in a higher extraction of ^{209}Po than ^{210}Po from unfiltered samples and, in turn, led to the calculation of lower ^{210}Po activities compared with the Co-APDC method: (1) the Fe(OH)$_3$ protocol did not quantitatively extract all of the dissolved ^{210}Po from seawater due to organic complexation; (2) siphoning of the supernatant from unfiltered samples precipitated with Fe(OH)$_3$ resulted in a loss of particles and associated ^{210}Po activity.

First, different chemical speciation between the natural ^{210}Po present in seawater and the artificial ^{209}Po added to the samples (in acid media) may prevent a complete equilibration between the isotopes over 9–24 h (**Supplementary Table 1**) and result in a differential extraction when precipitating with Fe(OH)$_3$. Little is known about the speciation of Po in seawater, but it may behave similarly to other group 16 metalloids, such as selenium (Stewart et al., 2008), which is predominantly found in organic form in surface seawater (Cutter and Cutter, 2001). Organic speciation of Po in seawater may arise through its distinctive biogeochemistry in which it is assimilated into organic matter and recycled with it. Previous studies have shown that ^{210}Po penetrates into the cytoplasm of bacteria and phytoplankton and associates with proteins and sulfur containing compounds in bacteria, phytoplankton and zooplankton (Fisher et al., 1983; Cherrier et al., 1995; Stewart and Fisher, 2003a,b). Therefore, at least some of the dissolved ^{210}Po atoms present in seawater, especially in the upper water column, would have likely been recycled and perhaps present as organic species. Further, Chuang et al. (2013) showed that Po is particularly prone to chelation by organic ligands like hydroxamate siderophores. Such organic speciation of ^{210}Po in seawater may reduce its adsorption onto iron hydroxides, whereas ^{210}Po would be effectively co-precipitated as a dithiocarbamate chelate with the Co-APDC method (Boyle and Edmond, 1975). If that was the case, regional differences in seawater chemistry and Po speciation would result in site-specific discrepancies between the Fe(OH)$_3$ and Co-APDC methods, in line with the results obtained in this study. In contrast, the ^{209}Po spike added to the acidified samples would not be speciated in the same way as natural ^{210}Po. After acidification and tracer addition, samples in the present study were allowed to equilibrate for 9–24 h before precipitation. This equilibration time, although typical of many studies using the Fe(OH)$_3$ method, may have been too short to destroy organic ligands. As a consequence, the ^{209}Po spike may not have completely equilibrated with natural ^{210}Po, leading to less scavenging of ^{210}Po than of ^{209}Po on iron hydroxides.

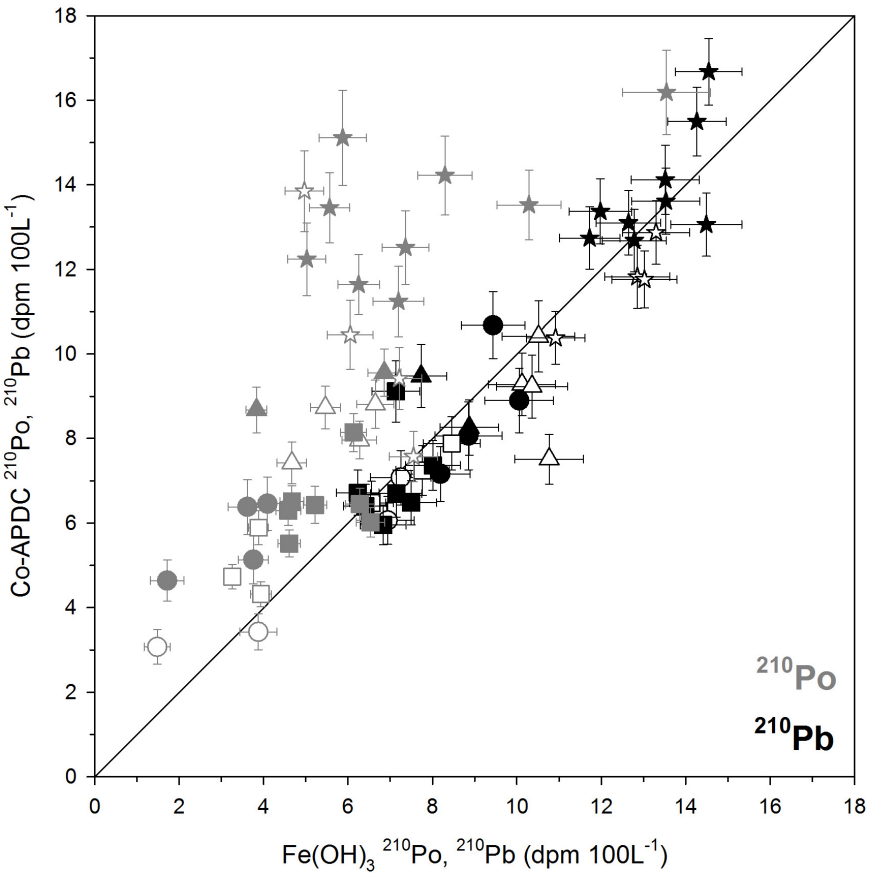

FIGURE 5 | Comparison of ^{210}Po (gray) and ^{210}Pb (black) determined by using the Co-APDC (*y*-axis) versus the Fe(OH)$_3$ (*x*-axis) methods. Symbols denote different study areas: IONIAN (triangles), CBN (squares), CBS (circles), and SOTS (stars). Open symbols show samples from the primary production zone, while closed symbols correspond to deeper samples. Solid line indicates 1:1 relationship.

Another possible explanation of the difference between the methods may be related to the fact that total (dissolved + particulate) ^{210}Pb and ^{210}Po activities were measured. Total seawater samples in the present study were acidified to pH 1–2 immediately after collection (see section "Duplicate Profiles of ^{210}Pb and ^{210}Po"). Marine biogenic particles typically have ^{210}Po/^{210}Pb activity ratios >1 (Cochran and Masqué, 2003), due both to adsorption of ^{210}Po onto particle surfaces and its incorporation into the particles. In contrast, ^{210}Pb is only adsorbed onto particle surfaces. As a consequence, ^{210}Po may not solubilize in an acidified sample over the 9–24 h allowed before precipitation. Samples processed with the Co-APDC method were filtered through 0.2 μm filters after precipitation and were subsequently digested with concentrated HNO_3, which would have effectively dissolved any particles in the sample along with the Co-APDC precipitate. For the samples precipitated with the Fe(OH)$_3$ method, most of the supernatant water was siphoned off at sea and the precipitate was returned to the laboratory with residual supernatant. Despite Fe(OH)$_{3\ \mathrm{TOT\ siph}}$ being a common procedure for the determination of total ^{210}Pb and ^{210}Po (see **Figure 1**), we suggest that this method may result in a loss of particles and associated ^{210}Po activity from the samples. If that was the case, the methodological offset between the total Fe(OH)$_3$ and Co-APDC protocols would depend on the particulate ^{210}Pb and ^{210}Po activities in seawater and vary as a function, for example, of place, time of year and phytoplankton biomass. Indeed, previous studies in the Mediterranean Sea and the Southern Ocean have reported that a significant fraction of the total ^{210}Po activity is associated with the particulate phase. For example, in the NW Mediterranean Sea, particulate ^{210}Po (>0.2 μm) activities in surface waters were reported to amount to 21% of the total activities (Masqué et al., 2002b). This agrees with an average of 19% of particulate ^{210}Po (>0.7 μm) measured at the DYFAMED site (NW Mediterranean Sea) from surface waters to >2400 m (unpublished results, P. Masqué). Similarly, in the Antarctic Circumpolar Current, the relative importance of particulate ^{210}Po (>1 μm) to total activities was on average 14% in the upper 600 m of the water column, including the sampling of phytoplankton blooms (Friedrich and Rutgers van der Loeff, 2002). These levels of particulate ^{210}Po comprise a significant fraction of the difference observed here between the Fe(OH)$_3$ and Co-APDC methods [28% for the Mediterranean Sea and 41% for

SOTS, see section "Direct Comparison of the $Fe(OH)_3$ versus Co-APDC Methods"]. It is important to emphasize that this potential bias would probably be unnoticeable for ^{210}Pb because particulate ^{210}Pb activities only amounted to 3–8% of the total activity in these studies (Friedrich and Rutgers van der Loeff, 2002; Masqué et al., 2002b), which are within the uncertainties associated with the ^{210}Pb measurements. However, the results from Friedrich and Rutgers van der Loeff (2002) and the DYFAMED site obtained by using the $Fe(OH)_{3\ DISS\ +\ PART}$ method showed a significant disequilibrium between total ^{210}Pb and ^{210}Po at depths ≥300 m (average total ^{210}Po/^{210}Pb activity ratio = 0.63 ± 0.05 and 0.79 ± 0.13, respectively). This suggests that a possible loss of particles when siphoning the supernatant from unfiltered samples precipitated with $Fe(OH)_3$ may not fully explain the differences observed between the two precipitation methods.

The compilation of ^{210}Pb and ^{210}Po studies shows that deficits of ^{210}Po at depth are more often observed when using $Fe(OH)_3$ versus Co-APDC, regardless of whether ^{210}Pb and ^{210}Po were analyzed on unfiltered or prefiltered seawater samples (**Figure 1**). This observation suggests that the organic complexation hypothesis may be the major explanation for the difference between methods. We acknowledge, however, that further experiments are needed in order to test other $Fe(OH)_3$ protocols and elucidate the underlying reasons behind the mismatch observed in this study. In particular, samples should be processed identically with respect to the treatment of the precipitate [filtered for both the $Fe(OH)_3$ and Co-APDC methods]. Thus, at this point, our findings cannot be extrapolated to other $Fe(OH)_3$ protocols, such as that used in the GEOTRACES program for the determination of ^{210}Pb and ^{210}Po in filtered seawater samples (Cutter et al., 2017).

Possible Overestimation of ^{210}Po-Derived Fluxes Using $Fe(OH)_3$

The comparison of methods presented in this study reveals that while $Fe(OH)_3$ and Co-APDC yield comparable results for ^{210}Pb, up to 40% lower ^{210}Po activities can be measured when using the $Fe(OH)_3$ method on unfiltered seawater samples. Moreover, unlike the iron hydroxide method, samples processed using Co-APDC showed radioactive equilibrium between ^{210}Pb and ^{210}Po at depth (see section "^{210}Pb and ^{210}Po Activities"), consistent with the long scavenging residence times in the deep ocean compared with the mean life of ^{210}Po.

The lower ^{210}Po/^{210}Pb activity ratios measured by using the $Fe(OH)_3$ method are apparent not only in deep samples, where large ^{210}Po deficits have been reported in multiple studies [most of them using $Fe(OH)_3$, **Figure 1**], but are also evident in samples from the euphotic zone and the upper twilight zone (**Figure 4**). This observation has important implications with respect to calculations of the export flux of POC (or other elements of interest) associated with sinking particles in the upper ocean. To evaluate these implications, we present the ^{210}Po-derived fluxes from a 1-D steady-state model (Equation 1), integrating the ^{210}Po deficits observed down to the PPZ depth for the duplicate samples processed by using $Fe(OH)_3$ and Co-APDC (**Figure 6**):

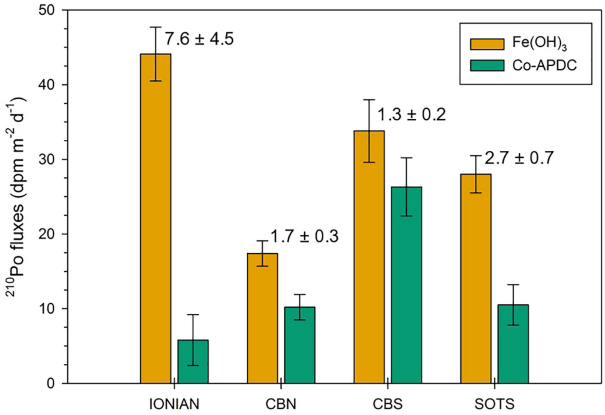

FIGURE 6 | ^{210}Po fluxes calculated from integrating the ^{210}Po deficit down to the base of the primary production zone using the $Fe(OH)_3$ (yellow) and Co-APDC (green) precipitation methods. Labels indicate the ratio between the $Fe(OH)_3$-derived to the Co-APDC-derived fluxes.

$$^{210}Po\ \text{flux} = \int_{PPZ}^{0} \lambda_{210Po} \left(^{210}Pb - {}^{210}Po\right) \quad (1)$$

where (^{210}Pb – ^{210}Po) is the integrated ^{210}Po deficit with respect to ^{210}Pb down to the depth of the PPZ (dpm m^{-2}) and λ_{210Po} is the decay constant of ^{210}Po (0.0050 d^{-1}). In addition to the PPZ depth, a relative light depth of 0.1% photosynthetically available radiation (PAR) could also be chosen as a reference depth to compare particle flux estimates from different sites (Buesseler et al., 2020b), but we only used the PPZ depth because we lack PAR data for some of the profiles.

The ^{210}Po fluxes obtained from our four duplicate profiles are shown in **Figure 6**. At CBS, the fluxes derived from $Fe(OH)_3$ and Co-APDC are similar within uncertainties (34 ± 4 and 26 ± 4 dpm m^{-2} d^{-1}, respectively). In contrast, for the Ionian Sea, CBN and SOTS profiles, export estimates from the $Fe(OH)_3$ method are a factor of 2 to 8 higher compared with Co-APDC estimates. This comparison clearly reveals how different conclusions can be drawn solely depending on the method used, where the $Fe(OH)_3$ method as applied here can lead to overestimated ^{210}Po fluxes. This suggests that ^{210}Po fluxes estimated from a commonly used $Fe(OH)_3$ protocol may be compromised to different degrees depending on the study area. The resulting exaggerated ^{210}Po flux would cause a proportional overestimation of the POC fluxes when multiplying the ^{210}Po flux by the POC/^{210}Po ratio associated with sinking particles.

CONCLUSION AND RECOMMENDATIONS

This study highlights that two commonly used methods for extracting ^{210}Pb and ^{210}Po from seawater can produce

different activities for ^{210}Po. On unfiltered seawater samples, precipitating ^{210}Pb and ^{210}Po with $Fe(OH)_3$ and siphoning off the supernatant shows total ^{210}Po activities up to 40% lower than those obtained with the Co-APDC method in which the precipitate is filtered. Deficits of ^{210}Po can be used to quantify POC fluxes and, therefore, the $Fe(OH)_3$ method may lead to artificially high ^{210}Po-derived POC fluxes. This finding has also important implications for understanding the behavior of Po in marine systems and defining possible new applications of this element to study biogeochemical cycles (e.g., sulfur).

Possible explanations for the lower ^{210}Po activities observed with the $Fe(OH)_3$ method include complexation of dissolved ^{210}Po in seawater preventing complete equilibration with the ^{209}Po tracer added to the samples, or the loss of particles when siphoning the supernatant from the samples. The compilation of ^{210}Pb and ^{210}Po studies presented here suggests that the former may be the major explanation for the difference between methods. Future research is needed to investigate whether longer sample storage after acidification and spiking allows more complete equilibration between natural ^{210}Po and the ^{209}Po tracer and gives results more comparable to those from the Co-APDC method. For these tests, we recommend using filtered seawater samples so that only the dissolved fraction is involved, and unfiltered seawater samples with filtration of the $Fe(OH)_3$ and Co-APDC precipitates. Processing a series of identical samples with increasing times for isotope equilibration before $Fe(OH)_3$ co-precipitation would allow determination of how quickly equilibration between ^{210}Po and ^{209}Po is reached. Laboratory experiments using natural seawater and seawater treated with ultra-violet irradiation (as done for trace metals), together with dissolved organic matter measurements on the samples, may also be useful to test the hypothesis that organic complexation of Po leads to differential extraction of the ^{209}Po spike and the *in situ* ^{210}Po when precipitating with $Fe(OH)_3$.

DATA AVAILABILITY STATEMENT

The original contributions presented in the study are included in the article/**Supplementary Material**, further inquiries can be directed to the corresponding author.

AUTHOR CONTRIBUTIONS

MR-M, VP, MC, NC, JG-O, and PM: contributed to conception and design. MR-M, VP, MC, and NC: contributed to the sampling and sample processing. MR-M, VP, MC, NC, JG-O, JKC, and PM: contributed to analysis and interpretation of data and drafted and revised the article. All authors contributed to the article and approved the submitted version.

FUNDING

MR-M was supported by an Endeavour Research Fellowship (6054) from the Australian Government, the Woods Hole Oceanographic Institution's Ocean Twilight Zone study, and the Ocean Frontier Institute. VP received funding from the Edith Cowan University under the Early Career Researcher Grant Scheme (G1003456) and the Collaboration Enhancement Scheme (G1003362). MC is currently funded by an ETH Zurich Postdoctoral Fellowship Program (17-2 FEL-30), co-funded by the Marie Curie Actions for People COFUND Program. Support to JKC was provided by the National Science Foundation grant OCE-1736591. The authors acknowledge the financial support from the Spanish Ministry of Science, Innovation and Universities through the "María de Maeztu" program for Units of Excellence (CEX2019-000940-M), the Australian Research Council LIEF Project (LE170100219), and the Generalitat de Catalunya (MERS; 2017 SGR-1588).

ACKNOWLEDGMENTS

We acknowledge the crew and scientists on board the B/O García del Cid, B/O Ángeles Alvariño, and R/V Investigator during the COSTEM (Ref. CMT2009-07806), MedSeA and IN2018_V02 expeditions, respectively. We are grateful to Patricia Cámara-Mor and Flavia Tarquinio for collecting and processing samples at sea at CBS and SOTS, respectively. We would like to thank Joan Manuel Bruach for his help over the years in the Environmental Radioactivity Laboratory (LRA, UAB). We also acknowledge discussions with Claudia Benitez-Nelson, Thomas Church, and Edward A. Boyle. We are also grateful to David Glover for his valuable advice on statistical analysis and to the reviewers and Ken Buesseler for their comments on earlier drafts. Finally, we thank the many authors who have shared their results with us to make the ^{210}Po/^{210}Pb compilation possible. The IAEA is grateful for the support provided to its Environment Laboratories by the Government of the Principality of Monaco.

SUPPLEMENTARY MATERIAL

The Supplementary Material for this article can be found online at: https://www.frontiersin.org/articles/10.3389/fmars.2021.684484/full#supplementary-material

REFERENCES

Anand, S. S., Rengarajan, R., Shenoy, D., Gauns, M., and Naqvi, S. W. A. (2018). POC export fluxes in the Arabian Sea and the Bay of Bengal: a simultaneous ^{234}Th/^{238}U and ^{210}Po/^{210}Pb study. *Mar. Chem.* 198, 70–87. doi: 10.1016/J.MARCHEM.2017.11.005

Bacon, M. P., Belastock, R. A., Tecotzky, M., Turekian, K. K., and Spencer, D. W. (1988). Lead-210 and polonium-210 in ocean water profiles of the continental shelf and slope south of New England. *Cont. Shelf Res.* 8, 841–853. doi: 10.1016/0278-4343(88)90079-9

Bacon, M. P., Brewer, P. G., Spencer, D. W., Murray, J. W., and Goddard, J. (1980a). Lead-210, polonium-210, manganese and iron in the Cariaco Trench. *Deep Sea Res. A Oceanogr. Res. Pap.* 27, 119–135. doi: 10.1016/0198-0149(80)90091-6

Bacon, M. P., Spencer, D. W., and Brewer, P. G. (1976). ^{210}Pb/^{226}Ra and ^{210}Po/^{210}Pb disequilibria in seawater and suspended particulate matter. *Earth Planet. Sci. Lett.* 32, 277–296. doi: 10.1016/0012-821X(76)90068-6

Bacon, M. P., Spencer, D. W., and Brewer, P. G. (1980b). "Lead-210 and polonium-210 as marine geochemical tracers: review and discussion of results from the Laborador Sea," in *Natural Radiation Environment III*, Vol. 1, eds T. F. Gesell and W. M. Lowder (Houston, TX: Technical Information Center/U.S. Department of Energy), 473–501.

Bam, W., Maiti, K., Baskaran, M., Krupp, K., Lam, P. J., and Xiang, Y. (2020). Variability in ^{210}Pb and ^{210}Po partition coefficients (Kd) along the US GEOTRACES Arctic transect. *Mar. Chem.* 219:103749. doi: 10.1016/J.MARCHEM.2020.103749

Boyd, P. W., Claustre, H., Levy, M., Siegel, D. A., and Weber, T. (2019). Multi-faceted particle pumps drive carbon sequestration in the ocean. *Nature* 568, 327–335. doi: 10.1038/s41586-019-1098-2

Boyd, P. W., and Trull, T. W. (2007). Understanding the export of biogenic particles in oceanic waters: is there consensus? *Prog. Oceanogr.* 72, 276–312. doi: 10.1016/j.pocean.2006.10.007

Boyle, E. A., and Edmond, J. M. (1975). "Determination of Trace Metals in Aqueous Solution by APDC Chelate Co-precipitation," in *Analytical Methods in Oceanography*, ed. T. R. P. Gibb (Washington, DC: American Chemical Society), 44–55. doi: 10.1021/ba-1975-0147.ch006

Buesseler, K. O., Benitez-Nelson, C. R., Roca-Martí, M., Wyatt, A. M., Resplandy, L., Clevenger, S. J., et al. (2020a). High-resolution spatial and temporal measurements of particulate organic carbon flux using thorium-234 in the northeast Pacific Ocean during the EXport Processes in the Ocean from RemoTe Sensing field campaign. *Elem. Sci. Anthr.* 8:030. doi: 10.1525/elementa.030

Buesseler, K. O., and Boyd, P. (2009). Shedding light on processes that control particle export and flux attenuation in the twilight zone of the open ocean. *Limnol. Oceanogr.* 54, 1210–1232. doi: 10.4319/lo.2009.54.4.1210

Buesseler, K. O., Boyd, P. W., Black, E. E., and Siegel, D. A. (2020b). Metrics that matter for assessing the ocean biological carbon pump. *Proc. Natl. Acad. Sci. U.S.A.* 117, 9679–9687. doi: 10.1073/PNAS.1918114117

Buesseler, K. O., Lamborg, C., Cai, P., Escoube, R., Johnson, R., Pike, S., et al. (2008). Particle fluxes associated with mesoscale eddies in the Sargasso Sea. *Deep Sea Res. 2 Top. Stud. Oceanogr.* 55, 1426–1444. doi: 10.1016/j.dsr2.2008.02.007

Ceballos-Romero, E., Le Moigne, F. A. C., Henson, S., Marsay, C. M., Sanders, R. J., García-Tenorio, R., et al. (2016). Influence of bloom dynamics on particle export efficiency in the North Atlantic: a comparative study of radioanalytical techniques and sediment traps. *Mar. Chem.* 186, 198–210. doi: 10.1016/j.marchem.2016.10.001

Cherrier, J., Burnett, W. C., and LaRock, P. A. (1995). Uptake of polonium and sulfur by bacteria. *Geomicrobiol. J.* 13, 103–115. doi: 10.1080/01490459509378009

Choi, H. Y., Stewart, G., Lomas, M. W., Kelly, R. P., and Moran, S. B. (2014). Linking the distribution of ^{210}Po and ^{210}Pb with plankton community along Line P, Northeast Subarctic Pacific. *J. Environ. Radioact.* 138, 390–401. doi: 10.1016/j.jenvrad.2014.02.009

Chuang, C.-Y., Santschi, P. H., Ho, Y.-F., Conte, M. H., Guo, L., Schumann, D., et al. (2013). Role of biopolymers as major carrier phases of Th, Pa, Pb, Po, and Be radionuclides in settling particles from the Atlantic Ocean. *Mar. Chem.* 157, 131–143. doi: 10.1016/j.marchem.2013.10.002

Chung, Y., and Finkel, R. (1988). ^{210}Po in the western Indian Ocean: distributions, disequilibria and partitioning between the dissolved and particulate phases. *Earth Planet. Sci. Lett.* 88, 232–240. doi: 10.1016/0012-821X(88)90080-5

Chung, Y., Finkel, R., Bacon, M. P., Cochran, J. K., and Krishnaswami, S. (1983). Intercomparison of ^{210}Pb measurements at GEOSECS station 500 in the northeast Pacific. *Earth Planet. Sci. Lett.* 65, 393–405. doi: 10.1016/0012-821X(83)90178-4

Chung, Y., and Wu, T. (2005). Large ^{210}Po deficiency in the northern South China Sea. *Cont. Shelf Res.* 25, 1209–1224. doi: 10.1016/j.csr.2004.12.016

Church, T., Rigaud, S., Baskaran, M., Kumar, A., Friedrich, J., Masqué, P., et al. (2012). Intercalibration studies of ^{210}Po and ^{210}Pb in dissolved and particulate seawater samples. *Limnol. Oceanogr. Methods* 10, 776–789. doi: 10.4319/lom.2012.10.776

Cochran, J. K., Bacon, M. P., Krishnaswami, S., and Turekian, K. K. (1983). ^{210}Po and ^{210}Pb distributions in the central and eastern Indian Ocean. *Earth Planet. Sci. Lett.* 65, 433–452. doi: 10.1016/0012-821X(83)90180-2

Cochran, J. K., and Masqué, P. (2003). Short-lived U/Th series radionuclides in the ocean: tracers for scavenging rates, export fluxes and particle dynamics. *Rev. Mineral. Geochemistry* 52, 461–492. doi: 10.2113/0520461

Cutter, G., Casciotti, K., Croot, P., Geibert, W., Heimbürger, L.-E., Lohan, M., et al. (2017). *Sampling and Sample-handling Protocols for GEOTRACES Cruises. Version 3.0*. Bremerhaven: GEOTRACES Standards and Intercalibration Committee, 139.

Cutter, G. A., and Cutter, L. S. (2001). Sources and cycling of selenium in the western and equatorial Atlantic Ocean. *Deep Sea Res. 2 Top. Stud. Oceanogr.* 48, 2917–2931. doi: 10.1016/S0967-0645(01)00024-8

De Soto, F., Ceballos-Romero, E., and Villa-Alfageme, M. (2018). A microscopic simulation of particle flux in ocean waters: application to radioactive pair disequilibrium. *Geochim. Cosmochim. Acta* 239, 136–158. doi: 10.1016/J.GCA.2018.07.031

Fisher, N. S., Burns, K. A., Cherry, R. D., and Heyraud, M. (1983). Accumulation and cellular distribution of ^{241}Am, ^{210}Po and ^{210}Pb in two marine algae. *Mar. Ecol. Prog. Ser.* 11, 233–237.

Fleer, A. P., and Bacon, M. P. (1984). Determination of ^{210}Pb and ^{210}Po in seawater and marine particulate matter. *Nucl. Instrum. Methods Phys. Res.* 223, 243–249. doi: 10.1016/0167-5087(84)90655-0

Flynn, W. W. (1968). The determination of low levels of polonium-210 in environmental materials. *Anal. Chim. Acta* 43, 221–227. doi: 10.1016/S0003-2670(00)89210-7

Friedrich, J., and Rutgers van der Loeff, M. M. (2002). A two-tracer (^{210}Po–^{234}Th) approach to distinguish organic carbon and biogenic silica export flux in the Antarctic Circumpolar Current. *Deep Sea Res. 1 Oceanogr. Res. Pap.* 49, 101–120. doi: 10.1016/S0967-0637(01)00045-0

Gascó, C., Antón, M. P., Delfanti, R., González, A. M., Meral, J., and Papucci, C. (2002). Variation of the activity concentrations and fluxes of natural (^{210}Po,^{210}Pb) and anthropogenic (^{239,240}Pu, ^{137}Cs) radionuclides in the Strait of Gibraltar (Spain). *J. Environ. Radioact.* 62, 241–262. doi: 10.1016/S0265-931X(01)00167-9

Hayes, C. T., Black, E. E., Anderson, R. F., Baskaran, M., Buesseler, K. O., Charette, M. A., et al. (2018). Flux of particulate elements in the North Atlantic Ocean constrained by multiple radionuclides. *Global Biogeochem. Cycles* 32, 1738–1758. doi: 10.1029/2018GB005994

Henson, S. A., Sanders, R., Madsen, E., Morris, P. J., Le Moigne, F., and Quartly, G. D. (2011). A reduced estimate of the strength of the ocean's biological carbon pump. *Geophys. Res. Lett.* 38:L04606. doi: 10.1029/2011GL046735

Hong, G. H., Baskaran, M., Church, T. M., and Conte, M. (2013). Scavenging, cycling and removal fluxes of ^{210}Po and ^{210}Pb at the Bermuda time-series study site. *Deep Sea Res. 2 Top. Stud. Oceanogr.* 93, 108–118. doi: 10.1016/j.dsr2.2013.01.005

Horowitz, E. J., Cochran, J. K., Bacon, M. P., and Hirschberg, D. J. (2020). ^{210}Po and ^{210}Pb distributions during a phytoplankton bloom in the North Atlantic: implications for POC export. *Deep Sea Res. 1 Oceanogr. Res. Pap.* 164, 103339. doi: 10.1016/j.dsr.2020.103339

Hu, W., Chen, M., Yang, W., Zhang, R., Qiu, Y., and Zheng, M. (2014). Enhanced particle scavenging in deep water of the Aleutian Basin revealed by ^{210}Po-^{210}Pb disequilibria. *J. Geophys. Res. Oceans* 119, 3235–3248. doi: 10.1002/2014JC009819

Kadko, D., Bacon, M. P., and Hudson, A. (1987). Enhanced scavenging of ^{210}Pb and ^{210}Po by processes associated with the East Pacific Rise near 8°45'N. *Earth Planet. Sci. Lett.* 81, 349–357. doi: 10.1016/0012-821X(87)90122-1

Kim, G. (2001). Large deficiency of polonium in the oligotrophic ocean's interior. *Earth Planet. Sci. Lett.* 192, 15–21. doi: 10.1016/S0012-821X(01)00431-9

Kim, G., and Church, T. M. (2001). Seasonal biogeochemical fluxes of ^{234}Th and ^{210}Po in the Upper Sargasso Sea: influence from atmospheric iron deposition. *Global Biogeochem. Cycles* 15, 651–661. 10.1029/2000GB001313

Ku, T.-L., and Lin, M.-C. (1976). ^{226}Ra distribution in the Antarctic Ocean. *Earth Planet. Sci. Lett.* 32, 236–248. doi: 10.1016/0012-821X(76)90064-9

Le Moigne, F. A. C., Villa-Alfageme, M., Sanders, R. J., Marsay, C., Henson, S., and García-Tenorio, R. (2013). Export of organic carbon and biominerals derived from ^{234}Th and ^{210}Po at the Porcupine Abyssal Plain. *Deep Sea Res. 1 Oceanogr. Res. Pap.* 72, 88–101. doi: 10.1016/j.dsr.2012.10.010

Lemaitre, N., Planchon, F., Planquette, H., Dehairs, F., Fonseca-Batista, D., Roukaerts, A., et al. (2018). High variability of particulate organic carbon export along the North Atlantic GEOTRACES section GA01 as deduced from ^{234}Th fluxes. *Biogeosciences* 15, 6417–6437. doi: 10.5194/bg-15-6417-2018

Ma, H., Yang, W., Zhang, L., Zhang, R., Chen, M., Qiu, Y., et al. (2017). Utilizing ^{210}Po deficit to constrain particle dynamics in mesopelagic water, western South China Sea. *Geochem. Geophys. Geosyst.* 18, 1594–1607. doi: 10.1002/2017GC006899

Maiti, K., Bosu, S., D'Sa, E. J., Adhikari, P. L., Sutor, M., and Longnecker, K. (2016). Export fluxes in northern Gulf of Mexico–comparative evaluation of direct, indirect and satellite-based estimates. *Mar. Chem.* 184, 60–77. doi: 10.1016/j.marchem.2016.06.001

Masqué, P., Isla, E., Sanchez-Cabeza, J. A., Palanques, A., Bruach, J. M., Puig, P., et al. (2002a). Sediment accumulation rates and carbon fluxes to bottom sediments at the western Bransfield Strait (Antarctica). *Deep. Res. 2 Top. Stud. Oceanogr.* 49, 921–933. doi: 10.1016/S0967-0645(01)00131-X

Masqué, P., Sanchez-Cabeza, J. A., Bruach, J. M., Palacios, E., and Canals, M. (2002b). Balance and residence times of ^{210}Pb and ^{210}Po in surface waters of the northwestern Mediterranean Sea. *Cont. Shelf Res.* 22, 2127–2146. doi: 10.1016/S0278-4343(02)00074-2

Matthews, K. M., Kim, C.-K., and Martin, P. (2007). Determination of ^{210}Po in environmental materials: a review of analytical methodology. *Appl. Radiat. Isot.* 65, 267–279. doi: 10.1016/J.APRADISO.2006.09.005

Moore, R. M., and Smith, J. N. (1986). Disequilibria between ^{226}Ra, ^{210}Pb and ^{210}Po in the Arctic Ocean and the implications for chemical modification of the Pacific water inflow. *Earth Planet. Sci. Lett.* 77, 285–292. doi: 10.1016/0012-821X(86)90140-8

Niedermiller, J., and Baskaran, M. (2019). Comparison of the scavenging intensity, remineralization and residence time of ^{210}Po and ^{210}Pb at key zones (biotic, sediment-water and hydrothermal) along the East Pacific GEOTRACES transect. *J. Environ. Radioact.* 198, 165–188. doi: 10.1016/J.JENVRAD.2018.12.016

Nozaki, Y., Ikuta, N., and Yashima, M. (1990). Unusually large ^{210}Po deficiencies relative to ^{210}Pb in the Kuroshio Current of the East China and Philippine seas. *J. Geophys. Res.* 95:5321. doi: 10.1029/JC095iC04p05321

Nozaki, Y., Zhang, J., and Takeda, A. (1997). ^{210}Pb and ^{210}Po in the equatorial Pacific and the Bering Sea: the effects of biological productivity and boundary scavenging. *Deep Sea Res. 2 Top. Stud. Oceanogr.* 44, 2203–2220. doi: 10.1016/S0967-0645(97)00024-6

Obata, H., Nozaki, Y., Alibo, D. S., and Yamamoto, Y. (2004). Dissolved Al, In, and Ce in the eastern Indian Ocean and the Southeast Asian Seas in comparison with the radionuclides ^{210}Pb and ^{210}Po. *Geochim. Cosmochim. Acta* 68, 1035–1048. doi: 10.1016/j.gca.2003.07.021

Owens, S. A., Pike, S., and Buesseler, K. O. (2015). Thorium-234 as a tracer of particle dynamics and upper ocean export in the Atlantic Ocean. *Deep Sea Res. 2 Top. Stud. Oceanogr.* 116, 42–59. doi: 10.1016/j.dsr2.2014.11.010

Puigcorbé, V., Roca-Martí, M., Masqué, P., Benitez-Nelson, C. R., Rutgers van der Loeff, M. M., Laglera, L. M., et al. (2017). Particulate organic carbon export across the Antarctic circumpolar current at 10°E: differences between north and south of the Antarctic Polar Front. *Deep Sea Res. 2 Top. Stud. Oceanogr.* 138, 86–101. doi: 10.1016/j.dsr2.2016.05.016

Rigaud, S., Puigcorbé, V., Cámara-Mor, P., Casacuberta, N., Roca-Martí, M., Garcia-Orellana, J., et al. (2013). A methods assessment and recommendations for improving calculations and reducing uncertainties in the determination of ^{210}Po and ^{210}Pb activities in seawater. *Limnol. Oceanogr. Methods* 11, 561–571. doi: 10.4319/lom.2013.11.561

Rigaud, S., Stewart, G., Baskaran, M., Marsan, D., and Church, T. (2015). ^{210}Po and ^{210}Pb distribution, dissolved-particulate exchange rates, and particulate export along the North Atlantic US GEOTRACES GA03 section. *Deep. Res. 2 Top. Stud. Oceanogr.* 116, 60–78. doi: 10.1016/j.dsr2.2014.11.003

Ritchie, G. D., and Shimmield, G. B. (1991). "The Use of ^{210}Po/^{210}Pb Disequilibria in the Study of the Fate of Marine Particulate Matter," in *Radionuclides in the Study of Marine Processes*, eds P. J. Kershaw and D. S. Woodhead (Dordrecht: Springer), 142–153. doi: 10.1007/978-94-011-3686-0_15

Roca-Martí, M., Puigcorbé, V., Friedrich, J., Rutgers van der Loeff, M. M., Rabe, B., Korhonen, M., et al. (2018). Distribution of ^{210}Pb and ^{210}Po in the Arctic water column during the 2007 sea-ice minimum: particle export in the ice-covered basins. *Deep Sea Res. 1 Oceanogr. Res. Pap.* 142, 94–106. doi: 10.1016/J.DSR.2018.09.011

Roca-Martí, M., Puigcorbé, V., Iversen, M. H., Rutgers van der Loeff, M. M., Klaas, C., Cheah, W., et al. (2017). High particulate organic carbon export during the decline of a vast diatom bloom in the Atlantic sector of the Southern Ocean. *Deep Sea Res. 2 Top. Stud. Oceanogr.* 138, 102–115. doi: 10.1016/j.dsr2.2015.12.007

Roca-Martí, M., Puigcorbé, V., Rutgers van der Loeff, M. M., Katlein, C., Fernández-Méndez, M., Peeken, I., et al. (2016). Carbon export fluxes and export efficiency in the central Arctic during the record sea-ice minimum in 2012: a joint ^{234}Th/^{238}U and ^{210}Po/^{210}Pb study. *J. Geophys. Res. Ocean.* 121, 5030–5049. doi: 10.1002/2016JC011816

Sarin, M. M., Bhushan, R., Rengarajan, R., and Yadav, D. N. (1992). Simultaneous determination of ^{238}U series nuclides in waters of Arabian Sea and Bay of Bengal. *Indian J. Mar. Sci.* 21, 121–127.

Sarin, M. M., Kim, G., and Church, T. M. (1999). ^{210}Po and ^{210}Pb in the South-equatorial Atlantic: distribution and disequilibrium in the upper 500 m. *Deep. Res. 2 Top. Stud. Oceanogr.* 46, 907–917. doi: 10.1016/S0967-0645(99)00008-9

Shimmield, G. B., Ritchie, G. D., and Fileman, T. W. (1995). The impact of marginal ice zone processes on the distribution of ^{210}Pb, ^{210}Po and ^{234}Th and implications for new production in the Bellingshausen Sea, Antarctica. *Deep Sea Res. 2 Top. Stud. Oceanogr.* 42, 1313–1335. doi: 10.1016/0967-0645(95)00071-W

Siegel, D. A., Buesseler, K. O., Doney, S. C., Sailley, S. F., Behrenfeld, M. J., and Boyd, P. W. (2014). Global assessment of ocean carbon export by combining satellite observations and food-web models. *Global Biogeochem. Cycles* 28, 181–196. doi: 10.1002/2013GB004743

Smith, J. N., Moran, S. B., and Macdonald, R. W. (2003). Shelf–basin interactions in the Arctic Ocean based on ^{210}Pb and Ra isotope tracer distributions. *Deep Sea Res. 1 Oceanogr. Res. Pap.* 50, 397–416. doi: 10.1016/S0967-0637(02)00166-8

Stewart, G., Cochran, J. K., Miquel, J. C., Masqué, P., Szlosek, J., Rodriguez y Baena, A. M., et al. (2007). Comparing POC export from ^{234}Th/^{238}U and ^{210}Po/^{210}Pb disequilibria with estimates from sediment traps in the northwest Mediterranean. *Deep Sea Res. 1 Oceanogr. Res. Pap.* 54, 1549–1570. doi: 10.1016/j.dsr.2007.06.005

Stewart, G., and Fisher, N. S. (2003a). Bioaccumulation of polonium-210 in marine copepods. *Limnol. Oceanogr.* 48, 2011–2019. doi: 10.4319/lo.2003.48.5.2011

Stewart, G., and Fisher, N. S. (2003b). Experimental studies on the accumulation of polonium-210 by marine phytoplankton. *Limnol. Oceanogr.* 48, 1193–1201. doi: 10.4319/lo.2003.48.3.1193

Stewart, G., Fowler, S. W., and Fisher, N. S. (2008). "The Bioaccumulation of U- and Th-Series Radionuclides in Marine Organisms," in *U-Th series nuclides in aquatic systems*, eds S. Krishnaswami and J. K. Cochran (Amsterdam: Elsevier Science), 269–305. doi: 10.1016/S1569-4860(07)00008-3

Stewart, G., Moran, S. B., and Lomas, M. W. (2010). Seasonal POC fluxes at BATS estimated from ^{210}Po deficits. *Deep Sea Res. 1 Oceanogr. Res. Pap.* 57, 113–124. doi: 10.1016/j.dsr.2009.09.007

Stewart, G., Moran, S. B., Lomas, M. W., and Kelly, R. P. (2011). Direct comparison of ^{210}Po, ^{234}Th and POC particle-size distributions and export fluxes at the Bermuda Atlantic Time-series Study (BATS) site. *J. Environ. Radioact.* 102, 479–489. doi: 10.1016/j.jenvrad.2010.09.011

Tang, Y., Castrillejo, M., Roca-Martí, M., Masqué, P., Lemaitre, N., and Stewart, G. (2018). Distributions of total and size-fractionated particulate ^{210}Po and ^{210}Pb activities along the North Atlantic GEOTRACES GA01 transect: GEOVIDE cruise. *Biogeosciences* 15, 5437–5453. doi: 10.5194/bg-15-5437-2018

Tang, Y., and Stewart, G. (2019). The ^{210}Po/^{210}Pb method to calculate particle export: lessons learned from the results of three GEOTRACES transects. *Mar. Chem.* 217:103692. doi: 10.1016/j.marchem.2019.103692

Thomson, J., and Turekian, K. K. (1976). ^{210}Po and ^{210}Pb distributions in ocean water profiles from the Eastern South Pacific. *Earth Planet. Sci. Lett.* 32, 297–303. doi: 10.1016/0012-821X(76)90069-8

van Beek, P., Sternberg, E., Reyss, J.-L., Souhaut, M., Robin, E., and Jeandel, C. (2009). ^{228}Ra/^{226}Ra and ^{226}Ra/Ba ratios in the Western Mediterranean Sea: barite formation and transport in the water column. *Geochim. Cosmochim. Acta* 73, 4720–4737. doi: 10.1016/J.GCA.2009.05.063

Verdeny, E., Masqué, P., Garcia-Orellana, J., Hanfland, C., Cochran, J. K., and Stewart, G. (2009). POC export from ocean surface waters by means of

^{234}Th/^{238}U and ^{210}Po/^{210}Pb disequilibria: a review of the use of two radiotracer pairs. *Deep Sea Res. 2 Top. Stud. Oceanogr.* 56, 1502–1518. doi: 10.1016/j.dsr2.2008.12.018

Verdeny, E., Masqué, P., Maiti, K., Garcia-Orellana, J., Bruach, J. M., Mahaffey, C., et al. (2008). Particle export within cyclonic Hawaiian lee eddies derived from ^{210}Pb–^{210}Po disequilibrium. *Deep Sea Res. 2 Top. Stud. Oceanogr.* 55, 1461–1472. doi: 10.1016/j.dsr2.2008.02.009

Wei, C.-L., Lin, S.-Y., Sheu, D. D.-D., Chou, W.-C., Yi, M.-C., Santschi, P. H., et al. (2011). Particle-reactive radionuclides (^{234}Th, ^{210}Pb, ^{210}Po) as tracers for the estimation of export production in the South China Sea. *Biogeosciences* 8, 3793–3808. doi: 10.5194/bg-8-3793-2011

Wei, C.-L., and Murray, J. W. (1994). The behavior of scavenged isotopes in marine anoxic environments: ^{210}Pb and ^{210}Po in the water column of the Black Sea. *Geochim. Cosmochim. Acta* 58, 1795–1811. doi: 10.1016/0016-7037(94)90537-1

Wei, C.-L., Yi, M.-C., Lin, S.-Y., Wen, L.-S., and Lee, W.-H. (2014). Seasonal distributions and fluxes of ^{210}Pb and ^{210}Po in the northern South China Sea. *Biogeosciences* 11, 6813–6826. doi: 10.5194/bg-11-6813-2014

Conflict of Interest: The authors declare that the research was conducted in the absence of any commercial or financial relationships that could be construed as a potential conflict of interest.

The reviewer WG declared a past co-authorship with the author NC to the handling editor.

The reviewer MRL declared a past co-authorship with several of the authors MR-M, NC, PM, VP to the handling editor.